Angular distribution of phonons from a planar heater in superfluid ^{4}He: Pressure and power dependence

D. H. S. Smith and A. F. G. Wyatt
School of Physics, University of Exeter, Exeter EX4 4QL, United Kingdom

(Received 7 August 2007; revised manuscript received 10 October 2007; published 20 December 2007)

We have measured the angular distribution of phonons propagating in liquid ^{4}He which are created by a planar heater. The angular distribution varies considerably with pressure in the range 0–20 bars. At small angles to the heater normal, the angular distribution shows a mesa shape at $P=0$. At $6<P<12$ bars a large cusplike peak replaces the mesa shape and the peak gradually disappears at higher pressures. At larger angles to the heater normal, the signal is very small at $P=0$ and grows slowly until $P\sim 15$ bars when it grows rapidly. At $P>19$ bars the overall angular distribution is cosinelike. The behavior is explained in terms of phonon interactions amongst the injected phonons, that take place in the liquid helium when there is anomalous phonon dispersion. The interactions change the energy of the phonons and this is detected by the phonon-energy sensitive bolometer. Modeling of the results indicates that at small angles to the heater normal, there is thermalization of the low energy phonons and the creation of high energy phonons, which decreases in the range $7.5<P<15$ bars. At larger angles to the heater normal, $>20°$, phonons with energy below the pressure-dependent critical energy only spontaneously decay. We find that the injected phonon spectrum can be approximately characterized by a Bose-Einstein spectrum with a temperature ~ 0.6 K, which is nearly independent of heater power.

DOI: 10.1103/PhysRevB.76.224519 PACS number(s): 67.40.Fd, 62.60.+v, 67.70.+n, 68.08.−p

I. INTRODUCTION

Many of the physical characteristics of superfluid ^{4}He can be well described in terms of its elementary excitations from a coherent ground state, which acts as a vacuum state for the excitations. The elementary excitations are phonons at low energies and both phonons and rotons at higher energies. As these are density fluctuations, which are essentially nonlinear, the excitations can interact with each other so that, among other things, they can come into thermal equilibrium. This paper continues our study of interactions between phonons in liquid ^{4}He; in particular how three phonon processes lead to either phonon decay or to an equilibrium anisotropic phonon system depending on phonon density.

A phonon pulse injected into liquid ^{4}He can either propagate ballistically without any interactions, or propagate as a strongly interacting system of phonons, as long as the temperature is so low that there is a negligible number of ambient phonons; this is typically 50 mK. The choice of behavior is determined by pressure; at $P>19$ bars there is ballistic propagation and at $P=0$ bars there are strong interactions.[1] In this paper we are interested in the phonon propagation at all pressures.

Pressure determines the phonon behavior because it varies the detailed shape of the dispersion curve as well as changing its gradient, i.e., the sound velocity.[2] The dispersion curve can be written as a function of momentum p, $\epsilon=cp[1+\psi(p)]$ where $|\psi(p)|\ll 1$. For pressures $P>19$ bars, $\psi(p)<0$ and the dispersion curve bends downwards from linear up to the maxon peak at $p/\hbar\sim 1$ Å^{-1}. For pressures $P<19$ bars the dispersion is anomalous: the dispersion curve initially bends upwards from linear before bending downwards. So $\psi(p)>0$ for $0<p<p_c$ and $\psi(p)<0$ for $p>p_c$, where p_c is the pressure dependent critical momentum defined by $\psi(p_c)=0$.[3–6]

This anomalous dispersion is small and can be estimated from the measured dispersion curve.[2] The maximum value of $\psi(p)$ is ~ 0.04 at $P=0$; it is smaller at higher pressures and is zero at $P=19$ bars. Nevertheless, the small positive value of $\psi(p)$ has an enormous effect on the phonons because it allows strong phonon scattering up to phonon energy ϵ_c, where ϵ_c corresponds to p_c, i.e., $\epsilon_c=cp_c$. At $P=0$, $\epsilon_c/k_B=10$ K. Strong small angle scattering, through the three phonon process (3pp),[7–9] occurs up to $\epsilon/k_B=8.7$ K,[10] where one phonon scatters to two phonons and vice versa. In the range $8.7<\epsilon/k_B<10$ K there are scattering processes where one phonon scatters to more than two phonons and vice versa. They have similar scattering rates to the 3pp rate.[10] We refer to all of them collectively as $1\leftrightarrow n$ processes. These fast processes cause either spontaneous decay if the phonon number density is low or thermalization if the phonon number density is high.

In solids, the acoustic phonon branches show normal dispersion, however, there can be strong three phonon processes due to scattering between the longitudinal and transverse branches. There can also be four phonon scattering but this is generally weaker than the three phonon scattering because 4pp requires higher order perturbation terms. The angles involved in 3pp scattering are in general not small because of the factor of $\sim 3/2$ in the ratio of the gradients of the longitudinal and transverse branches.[11] In contrast, the angles involved in 3pp scattering in liquid ^{4}He are small, because the three phonons are all on the same dispersion curve as only longitudinal phonons are allowed.

In liquid ^{4}He, when $\psi(p)<0$, the fastest allowed scattering process is the four phonon process (4pp).[12,13] This process conserves the phonon number with two incoming phonons creating two outgoing phonons, so no spontaneous decay is allowed by this process. The scattering rate for 4pp is much lower than for 3pp.[14,15] In the time scale of the

phonon propagation experiments, typically 50 μs, there is no thermalization due to 4pp. Furthermore, a phonon with $p > p_c$, has a lifetime which is only limited by the helium sample dimensions when there are no thermal phonons, because it then cannot scatter by 4pp.

When the dispersion is anomalous and the phonon system is strongly interacting by $1 \leftrightarrow n$ processes, there is still a lower rate of 4pp scattering within the phonon system. This is not wholly overshadowed by the $1 \leftrightarrow n$ scattering because one of the consequences of 4pp is to create phonons with energy $\epsilon > \epsilon_c$,[16,17] which is impossible by $1 \leftrightarrow n$ scattering. A phonon with $\epsilon > \epsilon_c$ has a lower group velocity than the pulse velocity of the interacting phonons,[2,18] and if the pulse is short, so that the phonon with $\epsilon > \epsilon_c$ does not scatter before it reaches the back of the pulse, then it is lost from the pulse.[17] Once this happens the $\epsilon > \epsilon_c$ phonon has a negligible probability of scattering with other such phonons, and it propagates ballistically behind the interacting pulse.

The effect of this process can be clearly seen in the signal from a short heater pulse $t_p \sim 100$ ns after it has traveled a distance of order 17 mm;[21] see also Fig. 2. The signal shows two peaks, the first peak is due to the strongly interacting phonons which travel at very nearly the velocity of sound, and the second and broader peak is due to phonons with $\epsilon > \epsilon_c$.

Such behavior has been investigated experimentally[19–23,1] and analyzed theoretically.[16,17,24–27] The strongly interacting phonons have a low energy, typically $\epsilon/k_B \sim 1$ K, and are called l phonons. The $\epsilon > \epsilon_c$ phonons are concentrated at $\epsilon \sim \epsilon_c(P)$.[23,24] These are relatively high energy phonons and are called h phonons.

When a high density of phonons is injected into the liquid ^{4}He at $P=0$, the phonons scatter by $1 \leftrightarrow n$ processes so rapidly that within 10 ns a new distribution has formed and all memory of the injected spectrum has been lost.[28] The phonons form a new quasiequilibrium distribution which can be pictured as a conical segment cut from an isotropic distribution in momentum space at temperature T_p.[16] The initial temperature T_p is thought to be <0.9 K, and the cone angle θ_c is typically 7°,[29] so the distribution has a net momentum along the heater normal. The cone of occupied states in momentum space has a solid angle Ω_p, where $\Omega_p = 2\pi(1-\cos\theta_c)$.

The exact description of the quasiequilibrium is a modified Bose-Einstein distribution where the ϵ/k_BT term for an isotropic distribution is replaced by $(\epsilon - \mathbf{p}\cdot\mathbf{u})/k_BT$ where $\mathbf{p}$ is the momentum of the phonon and $\mathbf{u}$ is a "drift" velocity of the phonon system along the axis of symmetry.[25] It can be seen that the anisotropic distribution function is defined by two parameters T and $\mathbf{u}$, whereas the isotropic one is defined only by T. The value of $\mathbf{u}$ is typically $0.98c$ where c is the sound velocity and T is typically 0.04 K.[9] The close relationship between the parameters of the cone approximation (Ω_p, T_p) and the actual quasiequilibrium distribution $(\chi = 1 - u/c, T)$ is given in Ref. 9.

As the pressure is increased from $P=0$ the anomalous dispersion weakens and ϵ_c decreases, and by 19 bars $\epsilon_c = 0$.[5] The velocity difference between the l and h phonons decreases as pressure increases and the l- and h-phonon peaks become less separated in time, and by >6 bars they cannot be resolved; see Fig. 2.

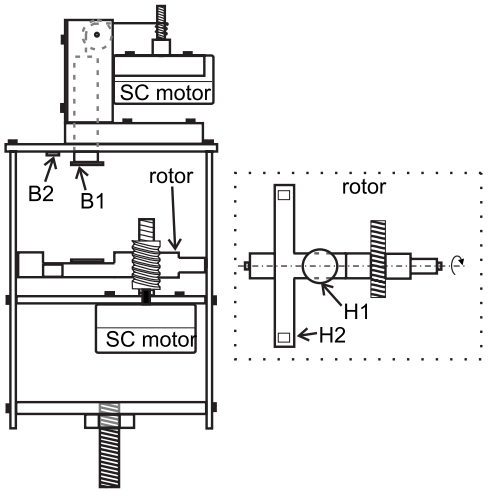

FIG. 1. Diagram of the apparatus. H1 and H2 are the heaters, and B1 and B2 are the bolometers, for the main experiment and for the angular measurements, respectively. H1 and H2 are mounted on a rotor driven by a superconducting stepping motor. The separation of H1 and B1 is 12.3 mm.

The angular distribution of the l phonons shows a distinctive behavior at 0 bars. The energy density is constant over an angle of ~5°, depending on heater power, from the normal to the heater, and at larger angles the energy density falls off sharply with increasing angle.[22] As h phonons are created in the region of high energy density, the angular distribution develops a mesa shape. This behavior indicates that the phonon pulse is strongly interacting within ~5° of the symmetry axis and, at larger angles, the phonon density is lower and hence the interaction rate decreases with angle.

The pressure dependence of the phonon signal along the normal to the heater shows a complex behavior showing first a maximum and then a minimum as pressure increases.[1] This behavior has not been explained in detail. Measurements at other angles to the heater are likely to help our understanding of the effect of pressure.

In this paper we present measurements of the angular distribution of the phonons from a planar heater with dimensions 1 mm × 1 mm at different pressures and for four heater powers. We present models of the signal at angles 0° and >20° to the heater normal. They give a good description of the main features of the measurements which allow us to draw some interesting conclusions about the thermalization of the low energy phonons and the creation of h phonons. We also obtain an estimate of the phonon spectrum injected by the heater.

II. EXPERIMENTAL ARRANGEMENT

The experimental arrangement is shown in Fig. 1. A thin film gold heater is mounted on the axis of a rotor with radial arms. The rotor can be rotated by a stepping motor which drives through a worm gear. The angle θ of the rotor is measured by timing phonon pulses from the heaters mounted

at the ends of the radial arms, to fixed detectors which are ~20 mm above them. In this way we obtain an angular accuracy of ~0.3°. The main detector is mounted on the end of a vertical bar which is directly above the heater. This bar can move vertically and is driven by a second stepping motor through a cotton thread connection. The cross section of the bar is square, and the bar moves through a square sectioned guide channel so that its end is laterally positioned. For the experiments reported in this paper, the heater bolometer distance was kept constant at 12.3 mm.

The thin film gold heater was evaporated onto a polished sapphire substrate 7.5 mm diameter and 0.4 mm thick. The opposite side of the sapphire disc was deliberately roughened so that it would diffusely reflect phonons from the heater pulse. This ensured that the phonon source for the experiment was a single pulse from the interface between the gold film and the liquid ^{4}He. In earlier experiments, we had suspected that the long and low-level tail to the measured phonon signal came from diffusive phonon propagation into the glass substrate. This energy would subsequently leak back into the gold film and emit phonons into the liquid ^{4}He after the end of the heating pulse. In sapphire the phonons propagate ballistically so this diffusive behavior should not occur. The tail was indeed absent with the sapphire substrate.

The detector was a zinc film evaporated on a polished sapphire substrate 10 mm diameter and 1 mm thick. The zinc film was scratched into a serpentine track over an area of 1 mm × 1 mm. A superconducting solenoid gave a magnetic field that held the zinc near its superconducting transition boundary. The bolometer was in a bridge with electronic feedback that maintained it at a constant resistance and hence temperature of ~0.35 K.[30–32] Recent experiments have shown that the sensitive area of the bolometer is actually only ~0.1 mm × ~0.1 mm.[29] It is most likely that the sensitive region is a single superconducting-normal boundary across the track width of ~0.1 mm.

The apparatus was sealed in a brass cell that was filled with ultrapure liquid ^{4}He,[33] and could be pressurized up to 24 bars. The pressure was measured with a Budenberg standard test gauge to an accuracy of 0.02 bars. The cell was mounted on a dilution refrigerator which maintained the temperature of the cell at ~50 mK during measurements.

The heater was pulsed by a Le Croy 9210 pulse generator with a repetition rate of 45 Hz. The signal was amplified with an EG and G 5113 preamplifier, and captured and averaged in a Tectronix DSA 601A to increase the signal to noise ratio.

III. RESULTS

Typical signals at different pressures, at $\theta=0$, are shown in Fig. 2. The peak signal at the l-phonon arrival time is measured as a function of angle θ from the heater normal, for heater powers 3.125, 6.25, 12.5, and 25 mW mm^{-2} into the 1 mm × 1 mm heater. The angular distributions, at a range of pressures, are shown in Fig. 3.

The angular distributions vary strongly with pressure. At $P=0$ bars, the angular distribution shows a mesa shape centered at $\theta=0$. The signal at $\theta>20°$ is very much smaller. At

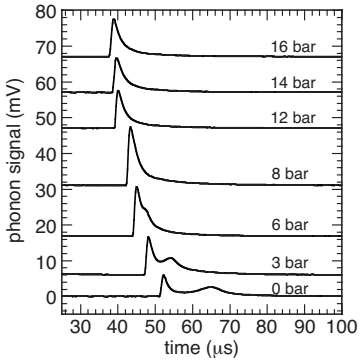

FIG. 2. Typical signals at different pressures at $\theta=0$, using H1 and B1. The first signal is from the l phonons and the broader second signal is due to h phonons. The heater pulse is 100 ns and 12.5 mW. Notice that the l- and h-signal peaks cannot be resolved at pressures above 6 bars.

$P=6$ bars, the mesa is replaced by a cusplike maximum which persists to $P=12$ bars. At $P=15$ bars the signal at $\theta=0$ has decreased but the $\theta>20°$ has grown so that the relatively small angular peak for $\theta<20°$ is on a broad cosinelike curve for $\theta>20°$. This trend continues to 17 bars. At $P=20$ and 24 bars there is only the cosinelike curve. The signal at $\theta>20°$ increases slowly with pressure up to $P\sim15$ bars and then rapidly up to $P=19$ bars, after which it is nearly constant.

The main effect of higher heater powers is to increase the signal proportionally to the heater power. However, at higher powers, the height of the cusplike peak at $P=6$ and 12 bars increases relative to the cosinelike curve at 20 and 24 bars. The results at 20 and 24 bars all show a slight depression in the angular range $-20°<\theta<0°$. We believe that this is an artefact, perhaps caused by some inhomogeneity in the heater.

The signal at $\theta=33°$ increases ~22 times from $P=0$ to $P=24$ bars, as shown in Fig. 4. The rate of increase with pressure is highest at $P\sim16$ bars. The behavior at the different heater powers is very similar which shows that the main effect of increasing heater power is to increase the phonon number density but to little change the energy dependence of the injected phonon spectrum. At 20 and 24 bars the signal divided by heater power shows a small decrease with power. This suggests that the fraction of energy going into the liquid ^{4}He, relative to that going into the heater substrate, decreases a little at higher powers.

The signal at $\theta=0°$ is shown in Fig. 5. The signal shows a strong increase in the range $0<P<7.5$ bars, a decrease in the range $7.5<P<15$ bars, an increase in the range $15<P<19$ bars, and, thereafter, remains constant. This is similar to the less detailed results published earlier.[1]

For $P>19$ bars, the injected spectrum of phonons propagates unchanged to the bolometer as $1\leftrightarrow n$ scattering is not possible and the 4pp scattering is very weak. This means that the angular dependence of the signal at 20 and 24 bars only depends on the angular emission from the heater. The measured cosinelike behavior is consistent with the transmission of phonons from the heater to the liquid ^{4}He via the background channel.[34] This is due to scattering at the surface of

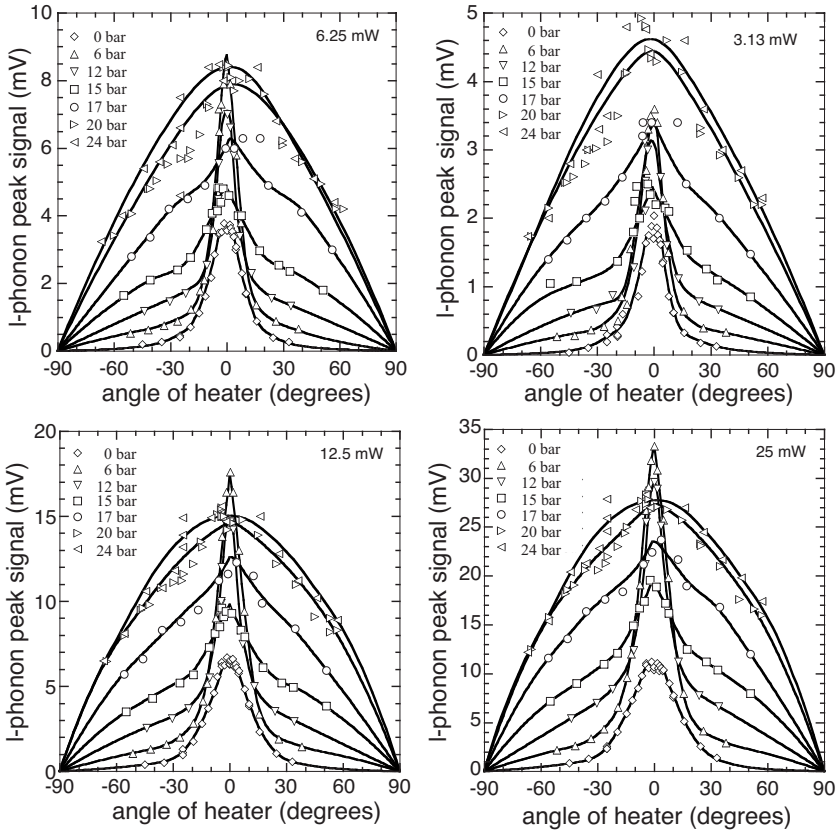

FIG. 3. The angular distribution of the signal, at the time of the *l*-phonon peak, at various pressures. The heater pulse is 100 ns and the heater powers in the panels are 3.125, 6.25, 12.5, and 25 mW.

the heater, so that a phonon in the heater creates two or more phonons in the liquid ^{4}He.[35] We see that there is no sign of an acoustic transmission channel which would give a narrow peak centered on $\theta=0$.[34] This is as expected because the gold film heater is rough; the acoustic channel is only seen with very flat and smooth interfaces, which have only been obtained by cleaving single crystals.[34,36]

The behavior at $P<19$ bars is due to two effects; the interaction of phonons and the change in the sensitivity of the bolometer with incident phonon energy.[37] These two effects can be seen to have a profound influence on the size of the signal, when one remembers that nearly the same energy is injected into liquid ^{4}He at all pressures.[1] For example, the small signal at low pressures and large angles is due to the decay of the phonons into many low energy phonons that have a very small transmission probability into the detector. As pressure increases, fewer phonons decay and a greater fraction of the phonon energy is in higher energy phonons which have a higher transmission probability into the detector. The details are given in the following sections where we model the signals at $\theta>20°$ and $\theta=0$.

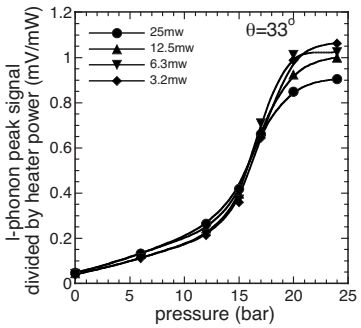

FIG. 4. The variation of the signal divided by heater power, at the time of the *l*-phonon peak and at an angle of $\theta=33°$, is shown as a function of pressure. The results for four powers are shown and it can be seen to first order that the signals scale with heater power.

IV. MODEL FOR $\theta>20°$

At angles $\theta>\sim 20°$ to the heater normal, the signal at low pressures is due to spontaneous decay of phonons, in

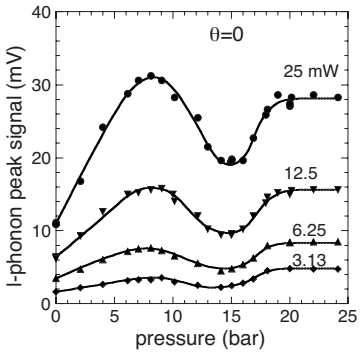

FIG. 5. The variation of the signal, at the time of the *l*-phonon peak and at the center of the angular distribution, $\theta=0$, is shown as a function of pressure. The results for four powers are shown and it can be seen to first order that the signals scale with heater power. The signal at the time of the *l*-phonon peak has some contribution from the *h* phonons, as described in the text.

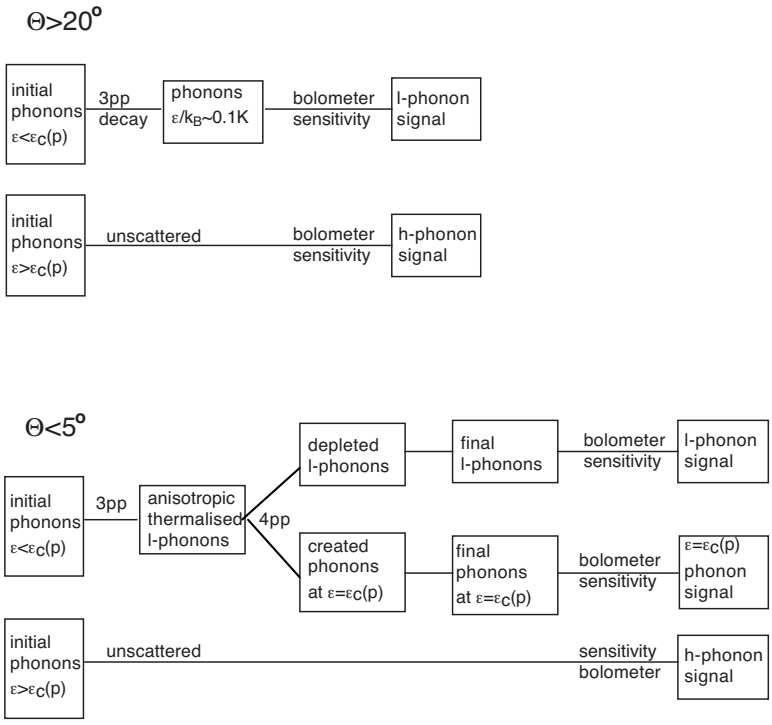

FIG. 6. A block diagram of the models for $\theta > 20°$ and $\theta < 5°$.

contrast to the strong phonon interactions which leads to rapid thermalization at $\theta < \sim 5°$. In other words, phonons with $\epsilon < \epsilon_c$, at $\theta > \sim 20°$, injected into the helium only decay in energy as they propagate to the detector, while at $\theta < \sim 5°$ there are roughly equal numbers of interactions which increase phonon energy as decrease it.

We model the pressure dependent signal at an angle $\theta > \sim 20°$ to the heater normal, in the way shown schematically in Fig. 6. The heater injects a spectrum of phonons into the liquid and we assume that the energy dependence of the spectrum can be characterized by temperature T_i, so the phonon number distribution function $n(\epsilon)$ is given by

$$n(\epsilon, T_i) = A \frac{\epsilon^2}{\exp(\epsilon/k_B T_i) - 1}, \tag{1}$$

where A determines the intensity of the spectrum which will vary with heater power and angle θ. The phonon energy density in the range ϵ to $\epsilon + d\epsilon$ is then $\epsilon n(\epsilon, T_i) d\epsilon$. The phonons with energy $\epsilon < \epsilon_c(P)$, where $\epsilon_c(P)$ is the maximum energy for spontaneous decay at pressure P, decay as they propagate to the detector. At zero pressure the decay rate is such that all these phonons decay to a low energy in the time it takes to reach the detector. At higher pressures the phonons also decay to a low energy as the theoretical spontaneous decay rate[7] is independent of the size of the upward dispersion as long as spontaneous decay is kinematically allowed, i.e., $\epsilon < \epsilon_c(P)$. We assume that phonons decay to $\epsilon/k_B = 0.1$ K. This low energy is necessary for the model to give a small signal at $P=0$. We discuss this assumption in the discussion section.

The phonons with energy $\epsilon > \epsilon_c(P)$ do not spontaneously decay, and, as there is an insignificant number of ambient thermal phonons in liquid ^{4}He at 50 mK to scatter them, they propagate to the detector with unchanged energies.

We use the values of $\epsilon_c(P)$ as a function of pressure as measured,[5] but slightly modified at low pressures so that $\epsilon_c(P=0)/k_B = 10$ K. This value is consistent with the dispersion curve as measured later.[2] Very approximately, $\epsilon_c(P)$ decreases linearly to zero at $P=19$ bars.

The sensitivity of the bolometer is an important factor in determining the final signal. The sensitivity is determined by the phonon transmission coefficient into the material of the detector, which in our case is zinc. The transmission coefficient is approximated by the function which linearly increases from the very small acoustic mismatch value at $\epsilon = 0$, to a value of 0.5 at $\epsilon/k_B = 5$ K and then remains constant at higher phonon energies.[37] This function is shown in Fig. 7.

The result of the model is shown in Fig. 8. At $P=0$, ϵ_c is at a much higher energy than the energy of the peak of the spectrum $\epsilon n(\epsilon, T_i)$, so almost all the phonons decay to low energies and the signal is low as the bolometer reflects most

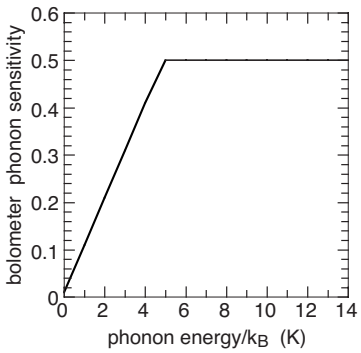

FIG. 7. The bolometer sensitivity is shown as a function of phonon energy (Ref. 37).

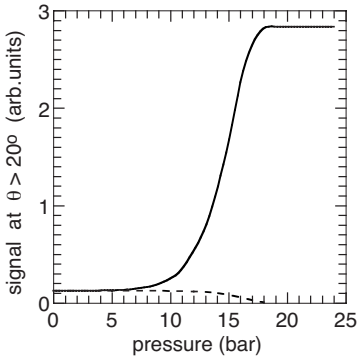

FIG. 8. The model result for the signal, at the time of the l-phonon peak and at $\theta > 20°$, is shown as a function of pressure by the solid line. The dotted line shows the contribution of the decayed phonons to the signal.

of these phonons. As P increases, the value of ϵ_c decreases and so more of the initial spectrum does not decay. The signal rises only slowly with pressure until $\epsilon_c(P)$ approaches the peak in the energy spectrum which is at $\epsilon/k_B \sim 2.86T_i$. As ϵ_c passes through the peak in the injected energy spectrum, the number of phonons that do not decay rises quickly and as these phonons have a high probability of transmission into the detector, the signal rises rapidly with pressure.

When $\epsilon_c(P)$ is on the low energy side of the peak in the energy spectrum, the signal changes slowly as very few phonons decay. The signal is independent of pressure when $\epsilon_c(P)=0$, i.e., for $P > 19$ bars, as then the injected spectrum propagates without change.

The model calculation, shown in Fig. 8, has $T_i=0.6$ K. The model reproduces the main features of the measurements shown in Fig. 4. The fastest rise in the model occurs at a pressure of ~15 bars which is slightly lower than the measured value of ~16 bars. The simple estimation of this pressure from the peak of the energy spectrum, $\epsilon n(\epsilon, T_i)$, at $\epsilon/k_B=1.7$ K gives the value of pressure as ~16.3 bars. This is an overestimation as it ignores the bolometer sensitivity decreasing for $\epsilon/k_B < 5$ K. If T_i is taken as 0.7 K, the model signal rises at a lower pressure which is in poorer agreement with the measured curves.

The ratio of the signals at 0 and 24 bars is 22.7 in the model and is measured to be 22, for heater power 12.5 mW. For $T_i=0.7$ K the model ratio is higher at 25.7. This again suggests that the value $T_i=0.7$ K is too high. At low pressures, $P < \sim 12$ bars, the model rises more slowly with pressure than the measurements; this is most likely due to the injected spectrum having more higher-energy phonons than a Bose-Einstein spectrum at 0.6 K. We conclude that the injected spectrum is nearly independent of heater power, in the range we have used, and it is only approximately described by a Bose-Einstein spectrum with $T_i \sim 0.6$ K.

V. MODEL FOR $\theta=0°$

We model the signal at the l-phonon arrival time, as a function of pressure in the following way. The cone approximation is implicitly used. The model is shown schematically in Fig. 6 labeled $\theta < 5°$. We first give an outline of the steps. The energy dependence of the injected spectrum is characterized by a temperature T_i. The energy that can thermalize, I_0, is the integral of $\epsilon n(\epsilon, T_i)$ for this spectrum, from $\epsilon=0$ to $\epsilon=\epsilon_c$. The injected phonons in the range $0 < \epsilon < \epsilon_c$ interact and form a new equilibrium distribution, whose energy dependence is characterized by a temperature T_{eff}. Only that part of the new spectrum with $\epsilon < \epsilon_c$ is used and the height of this truncated spectrum is scaled up so that the total energy is again I_0. During the propagation, some of the energy I_0 is converted to h phonons and this energy is put into h phonons with $\epsilon=\epsilon_c$.

The part of the injected spectrum with $\epsilon > \epsilon_c$ is not scattered and simply propagates unchanged to the detector. There are then three groups of phonons that arrive at the detector: the l phonons which are the interacting phonons with $\epsilon < \epsilon_c$; the created h phonons with energy $\epsilon=\epsilon_c$, and the unscattered phonons with $\epsilon > \epsilon_c$. The distribution of the total energy in these three groups strongly depends on pressure because ϵ_c decreases from $\epsilon_c/k_B=10$ K at 0 bars to $\epsilon_c/k_B=0$ K at 19 bars. The signal created by these groups of phonons is computed with the energy dependent phonon transmission coefficient which is shown in Fig. 7.

The model in more detail has the phonons with $\epsilon < \epsilon_c$ interacting strongly up to $P < 7.5$ bars, but from $7.5 < P < 15$ bars the thermalization of these phonons decreases and is zero at 15 bars. We effect this by decreasing the temperature of the thermalized phonons in the range $7.5 < P < 15$ bars by multiplying T_{eff} by a factor that decreases linearly from 1 at 7.5 bars to near zero at 15 bars, so that in the range $15 < P < 19$, $T_{eff}=0.05$ K. The intensity of the phonon spectrum is scaled up so that the total energy in these phonons, at a given pressure, is not changed. This assumed pressure dependence is suggested by the decrease in the 3pp interaction rate, as pressure increases and ϵ_c decreases, found theoretically.[9]

The fraction of the l-phonon energy going to h phonons, for $P < 7.5$ bars, is taken to be 0.5 at $\theta=0$. In the range of pressure $7.5 < P < 15$ bars we let this fraction decrease linearly to zero at 15 bars. This is similar to the measured decrease in h phonons with pressure.[1] In these measurements the h-phonon creation rate went to zero at 12 bars, however, there is a large uncertainty in this value of pressure and we find going to zero at 15 bars gives better agreement between the model and the present measurements. In particular, the minimum at 15 bars in the measured data, see Fig. 5, occurs at a lower pressure in the model if the h-phonon creation rate is zero at 12 bars. There is, at present, no theoretical calculation of the 4pp rate as a function of pressure.

We calculate $T_{eff}(P)$, at different pressures, by scaling from the value of T_{eff} at $P=0$ in the following way. The energy density in the phonon pulse is given by

$$E = \frac{\Omega_p \pi k_B^4 T_{eff}^4}{120 \hbar^3 c^3}, \tag{2}$$

where Ω_p is the occupied solid angle in momentum space. We see that E scales as T_{eff}^4/c^3. For an amount of energy E_n in a volume $A_n c t_p$, where A_n is the area of the pulse front and

t_p is the length of the heating pulse, the energy density is $E_n/A_n c t_p$, hence

$$\frac{E_n}{A_n c t_p} = E. \tag{3}$$

From Eqs. (2) and (3) we find $T_{eff}^4 \propto E_n c^2$ so T_{eff} is given by

$$\frac{T_{eff}(P)^4}{T_{eff}(P=0)^4} = \frac{I_0(P)c(P)^2}{I_0(P=0)c(P=0)^2}. \tag{4}$$

We choose the value of $T_{eff}(P=0)=0.6$ K for the following reasons. The only role of T_{eff} in the model is to define the spectrum of the interacting phonons when the pulse has propagated to the bolometer. Then the spectrum and the energy dependent transmission coefficient in the detector is used to calculate the signal. The model does not have to consider that the temperature of the pulse decreases as energy is given to the creation of h phonons, nor does it have to consider the temperature dependent rate of creation of h phonons. At $T_{eff}=0.6$ K the h-phonon creation rate is very low.[15] This value of T_{eff} makes the model results close to the measurements in this paper. In the model, T_{eff} is independent of the heater power. The pulse energy increases with heater power through Ω_p increasing.

$I_0(P)$ is calculated from the injected spectrum by the equation

$$I_0(P) \propto \int_0^{\epsilon_c(P)} \frac{\epsilon^3 d\epsilon}{[\exp(\epsilon/k_B T_i) - 1]c(P)^3}, \tag{5}$$

where $\epsilon_c(P)$ is from the measured dependence[5] but slightly modified to make $\epsilon_c(P=0)/k_B=10$ K. $T_{eff}(P)$ is calculated from Eq. (4) with values of $c(P)$ taken from Table A6 in Wilks.[38] We use $T_i=0.6$ K which is the same value as in the model for $\theta>20°$. It is a coincidence that T_i and $T_{eff}(P=0)$ have the same value.

The measured pressure dependence at $\theta=0$ is given in terms of the signal at the time of the peak in the l phonon signal. At $P=0$, the l phonons are well separated in time from the h phonons, so at this pressure the signal is predominately l phonons. However, as pressure increases, the time separation between the l and h phonon decreases, so an increasing proportion of the h-phonon signal arrives with the l phonons. We model this by including a linearly increasing proportion of the h-phonon signal from zero at $P=0$ to unity at $P>7$ bars.

The result of the model calculation is shown in Fig. 9 where we see it does reproduce the main features of the measured signal as a function of pressure. The rise in signal in the range of $0<P<7.5$ bars is due to the increasing proportion of the h-phonon signal at the l-phonon arrival time. The energies in the l- and h-phonon systems are nearly constant in this pressure range. The fall in signal in the range $7.5<P<15$ bars is mainly due to the decrease in the number and energy of the created h phonons but there is also a substantial decrease in the l-phonon signal for $10<P<15$ bars. The increase in the signal in the range $15<P<19$ bars is wholly due to phonons with $\epsilon>\epsilon_c$ in the injected spectrum, which are not scattered at all. The rapid increase is due to ϵ_c passing through the peak in the injected spectrum. When $P \geqslant 19$ bars, the entire injected spectrum reaches the detector and the signal is independent of pressure.

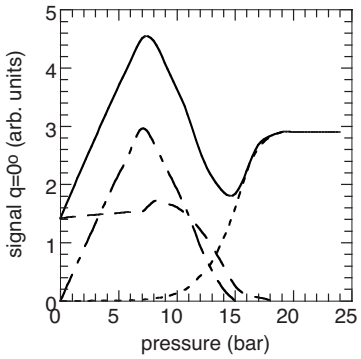

FIG. 9. The model result for the signal, at the time of the l-phonon peak and at $\theta=0$, is shown as a function of pressure. The solid line shows the total signal. The dash-dot line is the h-phonon contribution to the signal which peaks strongly at 7 bars; note that the h-phonon energy is constant for $0<P<7$ bars. The dashed line is the l-phonon contribution to the signal and is roughly constant until 10 bars. The weak maximum at 8 bars is due to the decrease in the energy going to h-phonons at this pressure. The dotted line is the $\epsilon>\epsilon_c$ phonon contribution to the signal which is injected by the heater. It rises strongly at around 15 bars.

VI. DISCUSSION

The main features of the measurements can be explained by considering how phonon interactions in liquid helium change the energy spectrum of the phonons from that which is injected by the heater, and the dependence of the transmission coefficient to the detector on phonon energy.

There are negligible phonon interactions at $P>19$ bars so the phonon spectrum that arrives at the detector is the same as that injected. The angular distribution is cosinelike and this reflects the angular dependence of the background channel of transmission from the heater into the liquid helium. As the heater surface is rough, the relatively small number of phonons in the acoustic transmission channel compared to the background channel are injected over a wide angle. At pressures $P<19$ bars there is $1 \leftrightarrow n$ scattering. For small angles, within $\sim 5°$ of the heater normal, the phonons are in a dynamic equilibrium, and for large angles $>20°$, the injected phonons undergo spontaneous decay. In the range $5° < \theta < 20°$ the strength of the thermalizing interactions diminish as θ increases due to the phonon density decreasing.

The $\theta>20°$ is less complex than the behavior at $\theta<5°$. Phonons decay if their energy is less than the critical energy $\epsilon_c(P)$ and the main dependence of their behavior on pressure comes from $\epsilon_c(P)$ decreasing as pressure increases. At low pressure, nearly all the injected phonons decay to low energies but, as pressure increases and $\epsilon_c(P)$ decreases, a larger fraction of the injected spectrum does not decay. As these phonons have $\epsilon>\epsilon_c(P)$ they have a higher energy and so create a relatively large signal compared to the decayed phonons. The signal rises quickest when $\epsilon_c(P)$ moves

through the peak of the injected spectrum. This happens at ~16 bars where $\epsilon_c(P)/k_B=2$ K so we know the peak in the injected spectrum is around ~2 K. However, the signal also depends on the energy dependent transmission coefficient which reduces the estimated value of the peak energy. We find that the injected spectrum is characterized by $T_i=0.6$ K which peaks at 1.7 K.

The behavior at $\theta<5°$ is dominated by the strong 3pp interactions that cause the l phonons to be in a dynamic equilibrium. This means that there is a small but significant high energy tail to the l phonon spectrum so that there are phonons with energies just less than ϵ_c. These phonons can scatter with low energy l phonons by the 4pp, and this can create phonons with energy $\epsilon>\epsilon_c(P)$.[16] The h phonons are lost from the l-phonon system if $ct_p<(c-v)\tau_4$,[16] where τ_4 is the inverse of the h-phonon scattering rate, i.e., for sufficiently short pulses, typically $t_p<10^{-7}$ s. The creation and loss of these h phonons depletes the energy of the l-phonon system and this lowers the temperature T_p of the l phonons and increases their occupied solid angle in momentum space.[26,27] The creation rate of h phonons is dominated by the temperature,[14,15] so the h phonons are created most rapidly near the heater and the creation rate drops as the l-phonon pulse propagates away from the heater.

At $P=0$ bars, the h-phonon pulse is well resolved from the l phonons, but as P increases more of the h phonons arrive at the time of arrival of the l phonons, and by $P>6$ bars, the peaks of the two pulses cannot be resolved. We attribute the increase in the signal at the l-phonon arrival time, in the range $0<P<7$ bars to the increasing contribution of the h phonons.

As the 4pp scattering rate has not been calculated as a function of pressure, we have to decide, for the modeling, how the creation of h phonons changes with pressure. We believe that the dominant effect is due to the degree of anomalous dispersion decreasing as P increases, i.e., $\psi(p)_{max}$ decreases and this reduces the angular range in the scattering integrals.[14] Experiments suggest that h-phonon creation ceases around 12 bars.[1] However, the minimum around 15 bars, see Fig. 5, is sensitive to the pressure at which the h-phonon creation stops; the cutoff for h-phonon production must be nearly at the same pressure as the minimum. As the minimum in $S(P)$ occurs at 15 bars, see Fig. 5, in the model we make the fraction of the l-phonon energy, that goes to the h phonons, linearly decrease from 7.5 bars to zero at 15 bars.

The 3pp interaction rate decreases with pressure due to the decrease in the anomalous dispersion.[9] This implies that the degree of thermalization of l phonons will also decrease with pressure. Again the measured minimum in the signal at ~15 bars indicates that the formation of an equilibrium l-phonon system must stop at $P\sim15$ bars. To incorporate this into the model, we make the temperature of the thermalized phonons decrease to nearly zero in the range $8<P<15$ bars. If the full thermalization extends to 17 bars, the minimum in the model disappears.

The fraction of injected phonons which do not scatter, i.e., those with $\epsilon>\epsilon_c(P)$, increases with pressure as $\epsilon_c(P)$ decreases. These phonons only make a small contribution to the signal until ϵ_c approaches the maximum in the injected energy spectrum. The rise in the measured signal $S(P)$ in the range $15<P<19$ bars is due to the rapid increase in these unscattered phonons. The minimum in the measured signal is sensitive to the energy of the maximum in the injected spectrum. As we define the spectrum in terms of a Bose-Einstein distribution function, we find that we need a temperature of $T_i=0.6$ K to get a rapid rise between 15 and 19 bars at both $\theta=0$ and $>20°$. A higher temperature means that the $\epsilon>\epsilon_c$ signal starts rising at a lower pressure and this rapidly makes the minimum in the model disappear.

So we see that the behavior of the measured data imposes tight limits on (i) the temperature of the injected spectrum, (ii) the h-phonon creation rate as a function of pressure and (iii) the decrease in the thermalization of the l phonons with increasing pressure. We hope that these results will stimulate theoretical work in these three areas.

The angular distribution shows a mesa shape at $P=0$ but this quickly becomes a cusplike peak by 6 bars which continues up to 12 bars. At $P>15$ bars, the peak structure becomes an increasingly small fraction of the total signal. The mesa shape has been attributed to the creation of h phonons which is such a strong function of temperature that it reduces the hot sector of the pulse, centered on $\theta=0$, to the same low temperature at which h-phonon creation is very low. This creates a region of constant energy density for $\theta<\sim5°$.[22] In these experiments we find that the final temperature is $T_{eff}\sim0.6$ K. As pressure increases the temperature T_{eff} increases a little, mainly due to the sound velocity decreasing; see Eq. (4).

A striking feature of the present measurements is the cusplike peak in the range $6<P<12$ bars. This is due to the h phonons which are included in the signal at the l-phonon arrival time. The narrow angular range of the cusplike peak shows that the h phonons are in a narrow angular range of momenta about the symmetry direction. This result agrees with the theoretical prediction of Adamenko, Kitsenko, Nemchenko, Slipko, and Wyatt.[26,27]

The details of the creation of the l-phonon pulse, from the injected phonons, which happens very near to the heater, has still to be understood. From the results of this paper, we have seen that the injected spectrum can be described by a temperature of 0.6 K. This only describes the shape as a function of energy and not its intensity. From the 20- and 24-bar data we know the injected spectrum is injected over a wide angular range with a cosinelike distribution. The characteristic temperature of the injected spectrum does not change much with heater power, but as the signal at $P>20$ bars scales with heater power, this indicates that the intensity of the injected spectrum scales with heater power.

The strongly interacting l-phonon pulse is formed from the injected spectrum hence the energy in the interacting pulse is proportional to the heater power. If the interacting pulse is described by the solid angle of the occupied states in momentum space Ω_p, as well as a temperature T_p, we have to consider how Ω_p and T_p change with heater power. There is only indirect evidence, as Ω_p and T_p have not been measured independently but all the measurements to date are consistent with the solid angle increasing approximately linearly with heater power and T_p increasing only a very little with power.

Such behavior is consistent with the measured energy in the pulse at ~17 mm from the heater at $P=0$ bars.[22] After

propagating this distance the central sector of the pulse has cooled to the same temperature, where h-phonon creation is negligible, for all heater powers. This happens because the h-phonon creation rate is a very strong function of temperature. So the increase in signal with heater power is not due to an increase in the final temperature. However, if the occupied solid angle in momentum space, Ω_p, is approximately linearly proportional to the heater power then the final energy density, and therefore signal, is proportional to Ω_p and hence heater power.

At the lowest power, the h-phonon contribution to the $\theta=0$ signal is smaller than at higher powers. This can be seen in the much smaller fractional rise, in the range $0<P<7.5$ bars, for the 3.13 mW curve in Fig. 5 compared to the curves at higher powers. This is most likely due to the decrease in the h-phonon creation rate at a slightly lower initial temperature of the l-phonon pulse.

Theory has explained how the l-phonon pulse propagates and creates h phonons, and so loses energy and momentum.[26,27] We assume in the model that half the energy in the l phonons, at $\theta=0$, is converted to h phonons. If energy ΔE is the energy given to the h phonons then the momentum given to the h phonons is $\sim\Delta E/c$. This is mainly along the symmetry axis as the h phonons are in a narrow momentum cone. The l phonons lose the same energy and momentum but as they are in a larger momentum cone, the cone angle, in the new equilibrium, must increase to lower the momentum by $\sim\Delta E/c$ along the symmetry axis. Also T_p decreases. In the correct distribution function, it is predicted that the "drift" velocity decreases and the temperature T increases,[26,27] which, on first encounter, is surprising. As yet there is no experiment that shows that the solid angle increases with propagation distance, however, it is clear from these experiments that the solid angle at 12.3 mm increases with heater power, because the final temperature is nearly independent of power but the signal increases with heater power. It is an open question how much of the increase in the solid angle occurs on the formation of the pulse and how much occurs as it propagates.

The detected signal depends on the phonon transmission coefficient into the zinc bolometer. We have used the phonon-energy dependence of transmission that has been determined.[37] This is satisfactory except perhaps at the lowest phonon energies. Theory[7] predicts that phonons will spontaneously decay to $\epsilon/k_B\sim0.25$ K in 12.3 mm. Phonons of this energy give too high a signal if the transmission coefficient rises linearly from the small acoustic value at $\epsilon/k_B=0$ to 0.5 at 5 K. As we see such a much lower signal, we conclude that either the phonons decay to a much lower energy than $\epsilon/k_B=0.25$ K, namely $\epsilon/k_B=0.1$ K which we used in the model, or the bolometer response is lower than we thought for 0.25 K phonons. At present there seems less doubt about the 3pp decay rate than the bolometer response to low energy phonons. This is a problem to be settled in the future.

VII. CONCLUSIONS

The measurements of the angular distribution of phonons from a planar heater at pressures in the range 0–24 bars, together with the modeling of the measured signals at $\theta=0$ and $>20°$, has allowed us to draw some important conclusions about the injected phonons and their subsequent behavior in the liquid ^{4}He.

At zero pressure, phonons emitted at small angles to the heater normal, $\theta<\sim5°$, strongly interact and form a dynamic equilibrium. The strength of the interactions diminishes with angle out to $\theta<\sim20°$. Phonons emitted at larger angles, $\theta>20°$, spontaneously decay. This is presumably because the phonon density in the pulse decreases as θ increases due to geometry.

The temperature of the injected phonons is ~0.6 K, and is largely independent of heater power; see Fig. 4. However, the intensity of the spectrum scales with heater power.

The temperature of the strongly interacting l phonons, at the bolometer, is found to be 0.6 K at $P=0$, which is a little lower than 0.7 K which was expected from the theoretical h-phonon creation rate.[17] However, there appears to be more higher-energy phonons than in a Bose-Einstein spectrum at a temperature of 0.6 K.

At $\theta=0$ the l phonons are thermalized for pressures 0–7.5 bars but are less than completely thermalized at higher pressures. The thermalization decreases to near zero by 15 bars.

At angles near to the heater normal and for pressures 0–7.5 bars, about half the energy in the l phonons, i.e., those with $\epsilon<\epsilon_c$ in the injected spectrum, goes to h phonons. From 7.5 to 15 bars the creation of h phonons decreases approximately linearly to zero.

The narrow cusplike peaks in the angular distribution at 6 and 12 bars show that the h phonons are created in a narrow cone in momentum space. This agrees with theory.[26,27]

For $\theta>20°$ the injected phonons with $\epsilon<\epsilon_c$ spontaneously decay to low energies and give little signal. The phonons with $\epsilon>\epsilon_c$ are not scattered and contribute nearly all the signal. This signal increases with pressure as $\epsilon_c(P)$ decreases with pressure and fewer phonons decay.

At $P>19$ bars, the dispersion curve is normal and the measured angular distribution is due to the angular distribution of the injected spectrum. This is due to the "background" channel of phonon transmission from the heater to the liquid ^{4}He, in which the energy of phonons is not conserved. This result is similar to earlier measurements.[34] There is no sign of transmission via the acoustic mismatch channel, which would give a narrow angular cone with a flat smooth interface. This is to be expected as the heater surface is rough. This shows that the narrow angle, over which strong interactions take place, has nothing to do with the acoustic mismatch cone.

ACKNOWLEDGMENTS

We thank R. V. Vovk for making the heaters and bolometers and C. D. H. Williams for use of his program for some data analysis.

[1] D. H. S. Smith, R. V. Vovk, C. D. H. Williams, and A. F. G. Wyatt, Phys. Rev. B **72**, 054506 (2005).
[2] W. G. Stirling, in *75th Jubilee Conference on Liquid Helium-4*, edited by J. G. M. Armitage (World Scientific, Singapore, 1983), p. 109; (private communication).
[3] H. J. Maris and W. E. Massey, Phys. Rev. Lett. **25**, 220 (1970).
[4] J. Jäckle and K. W. Kehr, Phys. Rev. Lett. **27**, 654 (1971).
[5] R. C. Dynes and V. Narayanamurti, Phys. Rev. Lett. **33**, 1195 (1974).
[6] A. F. G. Wyatt, N. A. Lockerbie, and R. A. Sherlock, Phys. Rev. Lett. **33**, 1425 (1974).
[7] S. Havlin and M. Luban, Phys. Lett. **42A**, 133 (1972).
[8] M. A. H. Tucker, A. F. G. Wyatt, I. N. Adamenko, A. V. Zhukov, and K. E. Nemchenko, Fiz. Nizk. Temp. **25**, 657 (1999) [Low Temp. Phys. **25**, 488 (1999)].
[9] I. N. Adamenko, K. E. Nemchenko, V. A. Slipko, Yu. A. Kitsenko, and A. F. G. Wyatt, Fiz. Nizk. Temp. **31**, 607 (2005) [Low Temp. Phys. **31**, 459 (2005)].
[10] I. N. Adamenko, Y. A. Kitsenko, K. E. Nemchenko, V. A. Slipko, and A. F. G. Wyatt, J. Phys.: Condens. Matter **18**, 10179 (2006).
[11] G. P. Srivastava, *The Physics of Phonons* (Adam Hilger, Bristol, 1990).
[12] I. M. Khalatnikov, *An Introduction to the Theory of Superfluidity* (Addison-Wesley, Redwood City, CA, 1989).
[13] M. A. H. Tucker and A. F. G. Wyatt, J. Phys.: Condens. Matter **4**, 7745 (1992).
[14] I. N. Adamenko, K. E. Nemchenko, and A. F. G. Wyatt, J. Low Temp. Phys. **25**, 1 (2001).
[15] I. N. Adamenko, K. E. Nemchenko, and A. F. G. Wyatt, J. Low Temp. Phys. **126**, 1471 (2002).
[16] I. N. Adamenko, K. E. Nemchenko, A. V. Zhukov, M. A. H. Tucker, and A. F. G. Wyatt, Phys. Rev. Lett. **82**, 1482 (1999).
[17] A. F. G. Wyatt, M. A. H. Tucker, I. N. Adamenko, K. E. Nemchenko, and A. V. Zhukov, Phys. Rev. B **62**, 9402 (2000).
[18] I. N. Adamenko, K. E. Nemchenko, V. A. Slipko, and A. F. G. Wyatt, J. Phys.: Condens. Matter **17**, 2859 (2005).
[19] M. A. H. Tucker and A. F. G. Wyatt, J. Phys.: Condens. Matter **6**, 2813 (1994).
[20] M. A. H. Tucker and A. F. G. Wyatt, J. Phys.: Condens. Matter **6**, 2825 (1994).
[21] M. A. H. Tucker and A. F. G. Wyatt, J. Low Temp. Phys. **113**, 621 (1998).
[22] R. V. Vovk, C. D. H. Williams, and A. F. G. Wyatt, Phys. Rev. B **68**, 134508 (2003).
[23] R. V. Vovk, C. D. H. Williams, and A. F. G. Wyatt, Phys. Rev. B **69**, 144524 (2004).
[24] I. N. Adamenko, K. E. Nemchenko, V. A. Slipko, and A. F. G. Wyatt, Phys. Rev. B **69**, 144525 (2004).
[25] I. N. Adamenko, Yu. A. Kitsenko, K. E. Nemchenko, V. A. Slipko, and A. F. G. Wyatt, Phys. Rev. B **72**, 054507 (2005).
[26] I. N. Adamenko, Yu. A. Kitsenko, K. E. Nemchenko, V. A. Slipko, and A. F. G. Wyatt, Phys. Rev. B **73**, 134505 (2006).
[27] I. N. Adamenko, Y. A. Kitsenko, K. E. Nemchenko, V. A. Slipko, and A. F. G. Wyatt, Low Temp. Phys. **33**, 387 (2007) [Fiz. Nizk. Temp. **33**, 523 (2007)].
[28] I. N. Adamenko, K. E. Nemchenko, A. V. Zhukov, M. A. H. Tucker, and A. F. G. Wyatt, Physica B **284-288**, 35 (2000).
[29] D. H. S. Smith, R. V. Vovk, C. D. H. Williams, and A. F. G. Wyatt, New J. Phys. **8**, 128 (2006).
[30] R. A. Sherlock and A. F. G. Wyatt, J. Phys. E **16**, 673 (1983).
[31] R. A. Sherlock, J. Phys. E **17**, 386 (1984).
[32] C. D. H. Williams, Meas. Sci. Technol. **1**, 322 (1990).
[33] P. C. Hendry and P. V. E. McClintock, Cryogenics **27**, 131 (1987).
[34] R. A. Sherlock, N. G. Mills, and A. F. G. Wyatt, J. Phys. C **8**, 300 (1975).
[35] A. F. G. Wyatt, and G. N. Crisp, J. Phys. (Paris), Colloq. **39**, C6-244 (1978).
[36] G. J. Page, R. A. Sherlock, A. F. G. Wyatt, and K. R. A. Ziebeck, in *Phonon Scattering in Solids*, edited by L. J. Challis, V. W. Rampton, and A. F. G. Wyatt (Plenum Press, London and New York, 1970), p. 18.
[37] T. W. Bradshaw and A. F. G. Wyatt, J. Phys. C **16**, 651 (1983).
[38] J. Wilks, *The Properties of Liquid and Solid Helium* (Clarendon Press, Oxford, 1967), p. 670.